[Article ID] 1003- 6326(2002)05- 0941- 06

Investigation on ductile fracture in fine-blanking process by finite element method①

LI Yu-ming (李昱明), PENG Ying-hong (彭颖红)
(National Die and Mould CAD Engineering Research Center, Shanghai Jiaotong University, Shanghai 200030, China)

[Abstract] In order to continuously analyze the whole fine-blanking process, from the beginning of the operation up to the total rupture of the sheet-metal, without computational divergence, a 3-D rigid visco-plastic finite-element method based on Gurson void model was developed. The void volume fraction was introduced into the finite element method to document the ductile fracture of the sheet-metal. A formulation of variation of the rigid visco-plastic material was presented according to the virtual work theory in which both the effects of equivalent stress and hydrostatic pressure in the deformation process were considered. The crack initiation of the sheet was predicted and the crack propagation was geometrically fulfilled in the simulation by separating the nodes according to the stress state. Furthermore, the influences of different state-variables on the deformation process were also studied.

[Key words] fine-blanking; ductile fracture; finite element method; Gurson plastic potential
[CLC number] TG 38 [Document code] A

1 INTRODUCTION

Sheet metal forming is a widely used process in manufacturing industries, among which fine-blanking process is the most advanced technique that offers an effective and economical metal cutting. Similar as all other blanking processes, fine blanking process ends in total rupture of the sheet metal as opposed at other processes such as stamping and drawing which are aimed at deforming the sheet plastically without rupture. At the same time, fine-blanking process is implemented with triple-action tools[1]: a punch, an indented V-ring, and an ejector to generate a concentrating compressive stress state and nearly pure shearing forces to perform a bulk deformation of the blank in the narrow clearance zone between the punch and the die. Comparing with the conventional blanking process and other metal forming processes, the material behavior in fine-blanking process is submitted to more complex stress and strain state, and is subject to ductile fracture and crack propagation phenomena[2].

The ductile fracture phenomena exist in many metal-forming processes, and the ductile fracture occurs when the material is subject to too large plastic deformation and stresses beyond the yield point. A lot of researches have been done on the ductile fracture by both experimental observations[3] and theoretical analysis[4~8]. However, the knowledge obtained so far of the ductile fracture is far to be sufficient and the related investigations in the fine-blanking process are much less, there is still much to do in this field as the ductile fracture plays an important role in the fine blanking process. Fine-blanking process can be broadly divided into three phases[9]. During the first phase the punch moves downward and elastic and plastic deformations take place. In the period of the second phase, the cutting edge of the punch penetrates the material and the deformation accumulates until the limit shear strength of the material is reached and the material is sheared along the cutting edge. The third phase consists of crack growth and propagation and the operation ends when the material is completely separated. From a numerical point of view, the main difficulty to simulate the fine-blanking process is to describe the material behavior continuously from the beginning of the operation up to the complete rupture. A good description of the above stages of fine-blanking process requires the development of reliable algorithms. Finite element method has recently been applied extensively in the numerical analysis and is proved to be a powerful means. There have been several investigations into the understanding of the mechanics of fine-blanking process[10~12], but these investigations did not consider the fracture and the studied problem was of two dimensions. Therefore, these investigations are not sufficient to clarify the mechanics of the process and haven't well simulated the bulk deformation. Based on the above situations, the purpose of this paper is to propose a 3-D finite element method that is capable of numerically analyzing all the phases of the fine-blanking process without computational divergence.

2 METHOD OF ANALYSIS

2.1 Modeling of ductile fracture

Accurate knowledge of the fracture process helps to select a suitable damage model. Numerous authors have studied different physical mechanisms leading to the final rupture[13~19]. It is well known that ductile

① [Received date] 2001- 10- 16; [Accepted date] 2001- 12- 29

fracture occurs on the micro-scale mainly by voids nucleation, growth and coalescence. In this study, the yield function proposed by Gurson[20], developed by Tvergarrd and Needleman[21~23] by introducing material constants q_1, q_2, and q_3 into the yield equation on considering the voids coalescence is written as:

$$\Phi_{GTN}(\sigma_{ij}, \sigma_M, f) = \left(\frac{\sigma_{eq}}{\sigma_M}\right)^2 - (1 + q_3 f^*(f)^2) + 2q_1 f^*(f)\cosh\left(\frac{q_2\sigma_{kk}}{2\sigma_M}\right) = 0 \quad (1)$$

where σ_{ij} is the average macroscopic Cauchy stress tensor, σ_M represents the equivalent tensile flow stress in the matrix material disregarding local stress variations, $\sigma_{eq} = \sqrt{(3/2)\, s_{ij}s_{ij}}$, is the macroscopic equivalent stress, where $s_{ij} = \sigma_{ij} - (1/3)\sigma_{kk}$, is the macroscopic Cauchy tress deviator, and f is the current void volume fraction. q_1, q_2, and q_3 are material constants and their values are here suggested as 1.5, 1.0, 1.5 respectively by Tvergarrd and Needleman.

Function $f^*(f)$ that models the material fracture is expressed as

$$f^* = \begin{cases} f & (f \leqslant f_c) \\ f_c + K_c(f - f_c) & (f_c < f \leqslant f_F) \\ 1/q_1 & (f > f_F) \end{cases} \quad (2)$$

where f_c is the value of void volume fraction when the connection of the voids start, f_F is the value of the void volume fraction when the material is fully damaged and K_c is the voids growth acceleration factor. When the void volume fraction f approaches f_F, the material locally loses its stress carrying capacity. The failure mentioned above is implemented in the numerical procedure by freezing the evolution of f after it reaches a value close to f_F, the condition $f = 0.95 f_F$ is used instead of $f = f_F$ because as $f \to f_F$ the macroscopic equivalent stress $\sigma_{eq} \to 0$ causing numerical difficulties.

The evolution of voids is presented by the commonly used strain controlled criterion[24, 25] which is proposed by Chu and Needleman[26]:

$$\dot{f} = (1 - f)\dot{\varepsilon}_{kk} + \frac{f_N}{s_N\sqrt{2\pi}} \cdot \exp\left[-\frac{1}{2}\left(\frac{\varepsilon_M^P - \varepsilon_n}{s_n}\right)^2\right]\dot{\varepsilon}_M^P \quad (3)$$

where f_N is the volume fraction of the uniformly distributed small size particles, s_n is the standard deviation of the distribution, $\dot{\varepsilon}_M^P$ is the equivalent plastic strain-rate of the matrix, and ε_n is a mean nucleation strain. The values of f_N, s_n, and ε_n are here set as 0.01, 0.1 and 0.3.

2.2 Formulation of variation

In this analysis a rigid viscous-plastic FEM is proposed, and the elastic effect is neglected. Based on the resolution of virtual work functional, the formulation of variation is expressed as: of all permissible kinematic compatible velocity fields $\boldsymbol{v}$ that satisfy the strain-rate velocity equations and the velocity boundary conditions at the loading surfaces, the real velocity field yields that the one-time functional of the work rate π is zero, that is

$$\delta\pi = 0 \quad (4)$$

and

$$\pi = \int_V \sigma_{eq}\dot{\varepsilon}_{eq}\,dV + \frac{1}{3}\int_V \sigma_m\dot{\varepsilon}_{kk}\,dV - \int_{S_\sigma} \boldsymbol{P}^T\boldsymbol{v}\,ds \quad (5)$$

where V is the plastic deformed volume of the material, $\dot{\varepsilon}_{eq}$ is the equivalent strain rate, σ_m is the average stress, $\boldsymbol{P}$ is the force vector on the given force surface S_σ. In the above formula, both the shearing force and the hydrostatic pressure are considered. The void volume fraction is integrated into this formulation by using the visco-plastic flow law:

$$\dot{\varepsilon}_{ij}^P = \dot{\Lambda}\frac{\partial\Phi_{GTN}}{\partial\sigma_{ij}} \quad (6)$$

where $\dot{\Lambda}$ is the visco-plastic multiplicative factor.

2.3 Matrix flow stress

The rigid viscous-plastic material is adopted in this analysis, and the isotropic flow stress of the matrix is assumed as

$$\sigma_M = C(\dot{\bar{\varepsilon}}_M)^m \quad (7)$$

where C is the material constant, m is the strain rate coefficient. The parameters of the chosen material are taken as $C = 814$MPa, and $m = 3.50$.

2.4 Modification of tool displacement

In the rigid visco-plastic finite element method, the speed of the tool is set constant in all iteration steps. Thus the current tool displacement of each iteration step depends on the time increment Δt of the current step. The time increment Δt is an important factor that determines the coordinates of the nodes and the state of the elements after each iteration step. In the rigid FEM, the time increment depends on the permissible volume loss rate, the most permissible strain and the stability of the convergence[27]. In this paper, the biggest time increment Δt_{max} is designated to satisfy the condition that the volume-loss rate is less than 3% and guarantee the convergence stability of the FE program.

The time increment Δt is dependent on two aspects:

1) Contact of the nodes and the tool boundary

In each iteration step, at most one node is allowed to touch the boundary of the tools. The shortest time that the nodes need to touch the boundary of the tools is denoted as Δt_1. If no node touch the boundary of the tools, $\Delta t_1 = \infty$.

2) Fracturing of elements

In each iteration step, at most one element is allowed to fracture. If one element fractures, $\int_0^{t+\Delta t_2} \dot{f}$

$dt = 0.95 f_F$, which means after Δt_2 from the beginning of the nth step, the element fractures. If no elements fracture, $\Delta t_2 = \infty$.

On considering both the above aspects, the time increment can be determined by the following formula:

If $\min(\Delta t_1, \Delta t_2) < \Delta t_{max}$, then $\Delta t = \min(\Delta t_1, \Delta t_2)$

else $\Delta t = \Delta t_{max}$

Therefore, the time increment may be modified for the needs of the boundary-contact of the nodes and of the fracture of the elements, and the tool displacement is therefore also modified.

2.5 Geometrical method of crack propagation

As we know, the material in the fine-blanking process is cut by shearing force and ends in separating under tensile stresses. The crack initiation and propagation are physically generated by the stresses. Therefore, the geometrical proceeding method of the crack initiation and propagation must take account the stress state. In this study, we adopt the nodes separating method to fulfill this aim. The method of separating nodes includes two cases:

1) If one element fractures mainly under shearing force, one of the nodes of this element whose shearing stress is the biggest is chosen to be separated into two nodes and the two newly generated nodes are set at a reasonable distance δ_1 from the original node in the direction which is vertical to the biggest shearing stress.

2) If one element fractures mainly under tensile force, one of the nodes of this element whose tensile stress is the biggest is chosen to be separated into two nodes and the two newly generated nodes are set at a reasonable distance δ_2 from the original node in the biggest tensile stress direction.

In both of the above situations, the volume of the newly generated crack is equal to the total volume of the voids contained in the neighboring elements. That is, the crack opening distances δ_1 and δ_2 are calculated according to the volume equilibrium of the elements which generate the crack. The balance of the nodal force of each node is satisfied in each step. Therefore when a node is separated, the distribution of the nodal force is not required.

3 FINITE ELEMENT APPROACH

The problem studied here is a bulk deformation. The shapes of most fine-blanking products are complex. Thus an analysis of all the deformed body costs much computing time and needs a computer of high quality. Therefore, a work-piece having a partially symmetric simplified form (see Fig. 1) is here studied in order to reduce the computing time and in the mean - time offer a 3 - D analysis . The two vertical

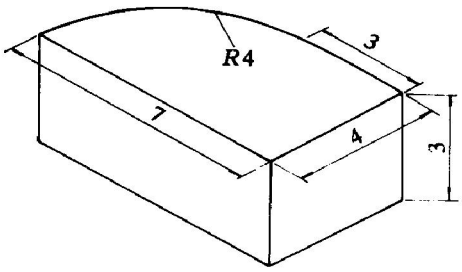

Fig. 1 One quarter of finished product

plains are the two symmetric plains.

The studied part and meshes are shown in Fig. 2. The blanking process is assumed to begin when the V-ring has already indented into the sheet material. The material outside the V-ring's tooth is considered in the numerical simulation as the material in this area nearly doesn't perform any deformation. In order to simplify the calculation, the undeformed material of the sheet is out of consideration in the numerical simulation. The outer boundary of the material under investigation is determined according to the V-ring's tooth and the outer vertical boundary goes through the V-ring's tooth. The assembly plan of the tools, the sheet and their geometrical data are shown in Fig. 3.

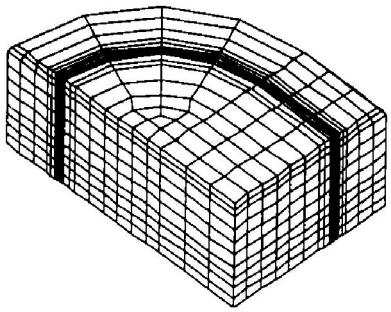

Fig. 2 Meshing of the studied sheet-metal

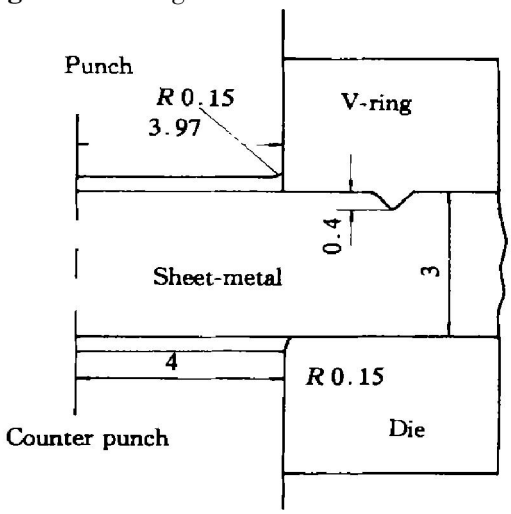

Fig. 3 Section of tool-assembly plan

4 DISCUSSION

A simulation of the fine-blanking process was carried out. Based on the simulation results, the dis-

tributions and the development of the state variables and of the ductile fracture as well as the crack propagation were studied.

Fig. 4 and Fig. 5 show the shapes of the deformed body when the punch penetrations into the sheet are 30% and 60% of the sheet thickness, respectively. The deformed body is remeshed when the punch penetration into the sheet is 55%. As shown in the figures, the meshes within the narrow zone of the clearance between the punch and the die are violently deformed and the material away from this zone is little deformed. Fig. 5 shows that crack generates within the clearance area of the tools and propagates along the diagonal line of the clearance.

Figs. 6, 7 and 8 illustrate the distributions of the state-variables: the void volume fraction, the equivalent stress and the equivalent strain, respectively.

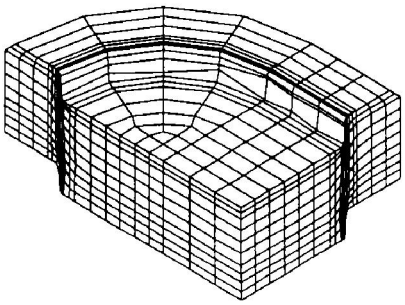

Fig. 4 Meshes of deformed body when punch penetration is 30% of sheet thickness

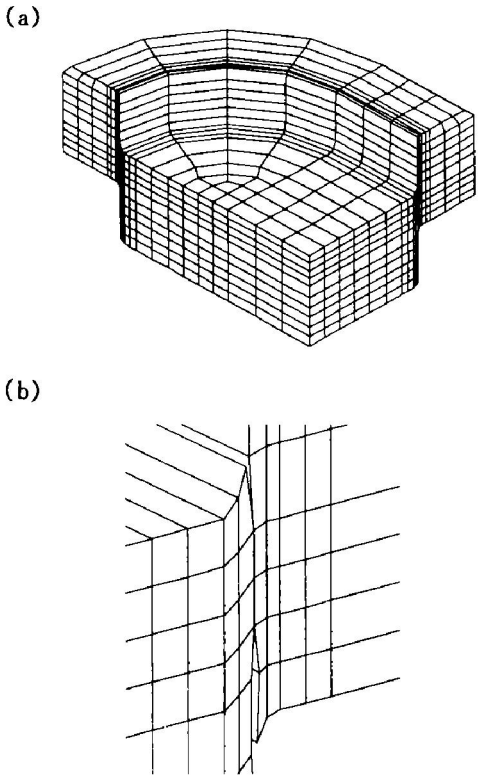

Fig. 5 Meshes of deformed body when punch penetration is 60% of sheet thickness
(a) —Global mesh;
(b) —Zoom view of clearance area of tools

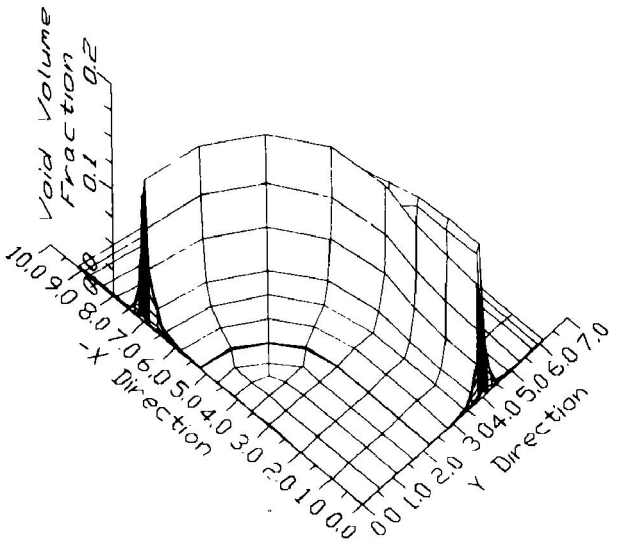

Fig. 6 Distribution of void volume fraction

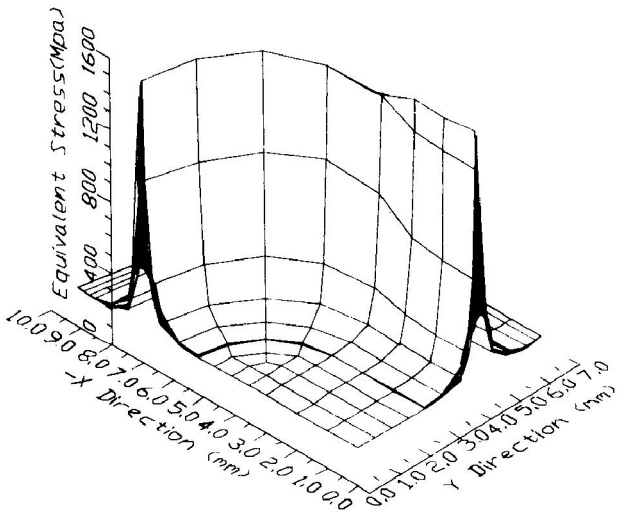

Fig. 7 Distribution of equivalent stress

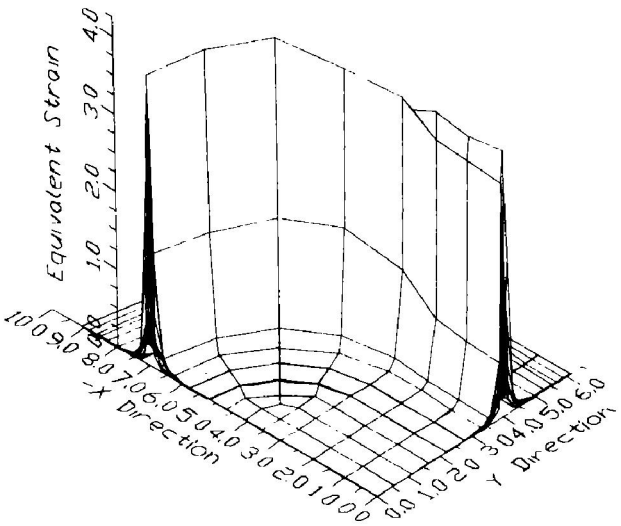

Fig. 8 Distribution of equivalent strain

From the distributions of the state-variables shown in the above diagrams, it is observed that all the state-variables increase abruptly within the narrow clearance between the punch and die. The nodes

of the meshespresenting the value of the state variables coincide with that of the deformed body's meshes. From the hidden meshes and the positions of the nodes, it is observed that all the biggest values of the state-variables are found on the free surfaces near the cutting edge of the tools and all the distributions of these diagrams are generally similar to each other.

In Fig. 6 the biggest void volume fraction value is located on the free surfaces near the cutting edges of the punch and the die where exist the largest tensile stress. This shows that the voids are sensible to the tensile stress and grow fast under tensile stress. The elements at this position firstly fracture and the crack appears, then the crack propagates into the material in the narrow clearance zone. Meanwhile, the growth speeds of the voids volume fraction on the arc segment, and on the line segment of the sheet are different. The growth speed on the arc segment is bigger than that on the line segment and the biggest value of void volume fraction is found at the middle part of the arc segment, because the curvature radius of the parts' contour has influence on the float of the metal during the deformation process. The arc segment is under bigger compressive stress state and has better plasticity, therefore is deformed more. Furthermore, at the conjunctive part of the arc segment and the line segment, the void volume fraction disturbs because of the change of the outline radius. All these phenomena show that the shape of the work-piece has influence on the void volume fraction growth.

Fig. 9 and Fig. 10 illustrate the development of the biggest void volume fraction and that of the punch force, respectively. Fig. 9 shows that as the punch penetrates the sheet, the deformation of the material increases, so does the biggest void volume. When the void volume fraction value reaches a certain value ($0.95f_F$), the crack initiates and when the element is fully fractured the void volume fraction does not increase any more. Fig. 10 shows the development of the punch force. When the punch penetration is about 30% of the sheet thickness, the punch force decreases abruptly. This is due to that at this moment some elements begin to fracture and lose their carrying capacity, resulting the softness of the elements and the initiation of the crack. During the stable cutting process afterwards, the punch force maintains at a certain level to continue the deformation of fine-blanking process. This phenomenon is in agreement with the experiments in Ref. [28].

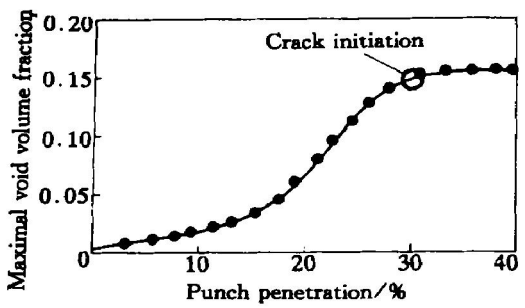

Fig. 9 Biggest void volume fraction vs punch penetration

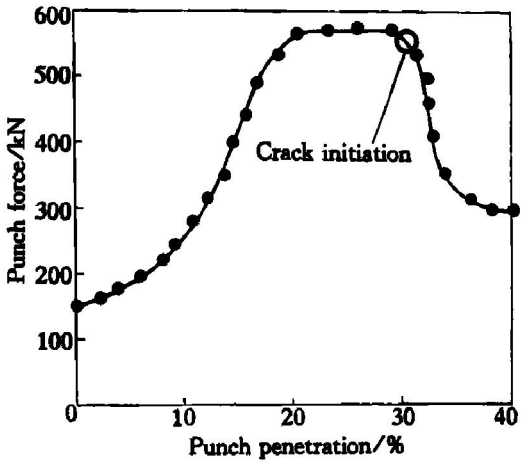

Fig. 10 Punch force vs punch penetration

5 CONCLUSIONS

1) To perform the fine-blanking process, the method of describing the material ductile fracture by means of voids volume fraction is appropriate.

2) In order to get accurate results, the displacement of the tool in the iteration step should be modified according to contact between nodes and the tools' boundary as well as the fracturing of the elements.

3) The propagation of the crack can be implemented geometrically by dividing the elements' nodes according to the stress state.

4) The material near the cutting edge of the tools firstly arrives at the critical void volume fraction value, leading to the initiation of the crack and then propagation into the material.

5) The shape of the work-piece has influence upon the distribution and development of the ductile fracture.

[REFERENCES]

[1] Lee T C, et al. Application of the finite-element deformation method in the fine blanking process[J]. Journal of Materials Processing Technology, 1997, 63: 744- 749.

[2] Hambli R. Finite element model fracture during sheet-metal blanking processes[J]. Engineering Fracture Mechanics, 2001, 68: 365- 378.

[3] Nagumo M, et al. Ductile crack growth resistance in hydrogen-charged steels[J]. Materials Transactions, 2001, 42: 132- 137.

[4] Vaz M Jr, Owen D R J. Aspects of ductile fracture and adaptive mesh refinement in damaged elasto-plastic materials[J]. International Journal for Numerical Methods in Engineering, 2001, 50; 29- 54.

[5] Ghosal A K, Narasimhan R. A finite element study of the effect of void initiation and growth on mixed-mode

ductile fracture[J]. Mechanics of Materials, 1997, 25: 113- 127.

[6] Kommori K. Simulation of chevron crack formation and evolution in drawing[J]. International Journal of Mechanical Sciences, 1999, 41: 1499- 1513.

[7] Hambli R. Finite element model fracture during sheet-metal blanking processes[J]. Engineering Fracture Mechanics, 2001, 68: 365- 378.

[8] Zhang K S, Bai J B, Francois D. Ductile fracture of materials with high void volume fraction[J]. International Journal of Solids and Structures, 1999, 36: 3407- 3425.

[9] Thomas P, Ralf J, Michael H. A finite element based model for the description of aluminum sheet blanking[J]. International Journal of Machine Tools and Manufacture, 2000, 40: 1993- 2002.

[10] Chan L C, et al. Experimental study on the shearing behavior of fine-blanking versus bar cropping[J]. Journal of Materials Processing Technology, 1998, 80- 81: 126- 130.

[11] Lee T C, et al. Further investigation of the fine-blanking process employing the large deformation theory[J]. Journal of Materials Processing Technology, 1997, 66: 258- 263.

[12] Chen Z H, et al. A study of strain localization in the fine-blanking process using the large deformation finite element method[J]. Journal of Materials Processing Technology, 1999, 86: 163- 167.

[13] Thomason P F. A three-dimensional model for ductile fracture by the growth and coalescence of micro-voids[J]. Acta Metal, 1985, 33(6): 1087- 1095。

[14] Li G C. Influence of seconary void damage in the matrix material around voids[J]. Fatigue Fracture Engineering Material Structure, 1989, 12(2): 105- 122.

[15] Zhang Z L. A new failure criterion for the Cursor-Tvergaard dilational constitutive model[J]. International Journal of Fracture, 1995, 70: 321- 334.

[16] Suhao, et al. Computer implementation of damage models by finite element and mesh-free methods[J]. Computer Methods in Applied Mechanics and Engineering, 2000, 187: 401- 440.

[17] Ghosal A K. A finite element study of the effect of void initiation and growth on mixed-mode ductile fracture[J]. Mechanics of Materials, 1997, 25: 113- 127.

[18] Zhang K S, Bai J B, Francois D. Ductile fracture of materials with high void volume fraction[J]. International Journal of Solids and Structures, 1999, 36: 3407 - 3425.

[19] Reddy N V, et al. Ductile criteria and its prediction in axisymmetric drawing[J]. International Journal of Material Tools & Manufacture, 2000, 40: 95- 111.

[20] Gurson A L. Continuum theory of ductile rupture by void nucleation and growth: Part 1. yield criteria and flow rules for porous ductile media[J]. ASME J Eng Mat Technl, 1977, 99: 2- 15.

[21] Tvergaard V. On localization in ductile materials containing spherical voids[J]. International Journal of Fracture, 1982, 18: 237- 252.

[22] Tvergaard V . Influence of voids on shear band instabilities under plane strain conditions[J]. International Journal of Fracture, 1981, 17: 389- 407.

[23] Tvergaard V, Needleman A. Analysis of the cup-cone fracture in a round tensile bar. Acta Metallurgica, 1984, 32: 157- 169.

[24] Samuel M. FEM simulations and experimental analysis of parameters of influence in the blanking process[J]. Journal of Materials Processing Technology, 1998, 84: 97- 106.

[25] Xu X P, Needleman A. Simulation of ductile failure with two scales of voids[J]. European Journal of Mechanics, A/Solids, 1991, 10: 459- 484.

[26] Chu C C, Needleman A. Void nucleation effects in biaxially stretched sheets[J]. J Eng Mater Tech, 1989, 102: 249- 256.

[27] ZHANG Xing-quan, et al. Simulation of cylindrical upsetting of porous materials by finite element method[J]. Trans Nonferrous Met Soc China, 1998, 8(1): 24- 27.

[28] Cold Forming and Fineblanking. FEINTOOL. 1997.

(Edited by YUAN Sai-qian)